

N63 12244

NASA TN D-1519

554141

B3 28



## TECHNICAL NOTE

D-1519

### THE EFFECT OF VACUUM ON THE PENETRATION CHARACTERISTICS OF PROJECTILES INTO FINE PARTICLES

By Leonard V. Clark and John Locke McCarty

Langley Research Center  
Langley Station, Hampton, Va.

**CASE FILE  
COPY**

NATIONAL AERONAUTICS AND SPACE ADMINISTRATION  
WASHINGTON

January 1963

NATIONAL AERONAUTICS AND SPACE ADMINISTRATION

---

TECHNICAL NOTE D-1519

---

THE EFFECT OF VACUUM ON THE PENETRATION CHARACTERISTICS  
OF PROJECTILES INTO FINE PARTICLES

By Leonard V. Clark and John Locke McCarty

SUMMARY

The penetration characteristics of various spherical projectiles impacting on to a test-bed material of fine particles were examined in a pressure environment which ranged from atmospheric to  $1 \times 10^{-5}$  mm Hg absolute. The investigation included measurements of the depth of penetration and analysis of the impact processes by photographic techniques to evaluate the effects of variations in the material particle size, testing technique, and the size, mass, and velocity of the impacting projectile.

The results of this investigation indicate that the depth of penetration into aluminum oxide particles ranging in size from 600 microns down to approximately 32 microns (granular material) is independent of both the environmental pressure and the average particle size. However, impacts into particles smaller than 32 microns (powdery material) indicate that the depth of penetration increases with decreasing particle size and is dependent upon the environmental pressure in the range between atmospheric and approximately 1 mm Hg. High-speed motion pictures taken during impacts on the powdery material revealed that the number of particles expelled during the impact decreased as the environmental pressure was reduced from atmospheric to approximately 1 mm Hg. No expulsion was evident at lower pressures.

INTRODUCTION

The subject of this paper is believed to be of special interest in connection with various conceptions of the lunar surface. Of primary importance to manned lunar flight is the ability of the vehicle upon landing on the moon to remain on the surface in a position acceptable for surface operations and relaunch to earth. The design of a vehicle to land on the lunar surface is highly dependent on the nature of that surface. If the surface is firm and fairly level, the solution of the landing and take-off problem is rather straightforward. However, should the surface consist of deep layers of dust, the landing and take-off problem could be complicated by surface erosion and dust entrainment by the retro-rocket. In addition, the presence of dust introduces a potentially dangerous environment inasmuch as such a surface may not offer sufficient bearing strength to support the vehicle in a tenable position.

Reliable data on the nature of the lunar surface are needed for engineering purposes as well as to satisfy scientific curiosity. Although the data on the nature of the lunar surface are very limited, there are many opinions by astronomers and other scientists (for example, refs. 1 to 3) as to the presence of dust on the lunar surface. However, scientists, in general, disagree as to its formulation, quantity, distribution, behavior, and particle size. For example, controversy regarding the dust behavior ranges from the assumption that the lunar dust is in a fluid state to the assumption that the surface is in the form of a sintered mass. In the one extreme, it is argued that dust from the high regions is transported to the low regions by such mechanisms as electrostatic forces and micrometeorite explosions, whereas, at the other extreme, it is argued that the dust is sintered as a result of the immoderate lunar environment (high vacuum, extreme temperature, solar radiation, etc.) and, as such, is void of any migratory tendencies. These and other such arguments very naturally promote variations in the predicted depths of the dust layer and in the predicted sizes of the dust particles. From such theories, it appears that the dust layer, if it exists, can be expected to range in depth from several millimeters on the higher regions to over a kilometer on the lower regions of the surface. Recent radar, photometric, and thermal radiation measurements, summarized in references 4 and 5 and in other papers suggest shallow depths. With some exceptions, the estimated dust particle sizes, based on measurements of electromagnetic radiation in the infrared, visible, radio, and radar bands, range from 10 to 300 microns.

Until the nature of the lunar surface is adequately known, the design requirements for placing payloads intact on the lunar surface must include the effects of a wide range of possible landing surfaces. In view of the dust concept, considerable attention must be given to the characteristics of bodies landing or impacting in dust-like media in a lunar environment. One primary characteristic, dictated by the attitude and positioning requirements of the communication, scientific exploration, and recovery systems, is the depth to which bodies will penetrate the surface upon landing. Reference 6 presents the results of a study of the penetration of hemispherical nose projectiles in various materials including sand and references other impact studies in that medium. However, the tests of these studies were performed under atmospheric conditions and possibly do not reflect penetration characteristics which would prevail under the environmental conditions which exist at the lunar surface. The behavior of bodies impacting various media under such an environment is virtually unknown. To the authors' knowledge, the available literature consists of four references which discuss the results of penetration tests in dust-like media under vacuum pressures. References 7 and 8 present the results of limited studies of penetration into fine particles at atmospheric and at slight vacuum pressure. Reference 9 presents the results of a more recent study wherein penetration depths in several volcanic-type dusts were examined over a wider range of vacuum pressure, but where the test media were shallow in depth, contained mixed particle sizes, had been packed, and in all cases (including tests under atmospheric pressure) had been subjected to the lowest test vacuum pressure. Reference 10 presents the results of a recent and more comprehensive study of penetration in crushed olivine basalt under atmospheric and vacuum pressure environments; the test media consisted of random-particle-size mixtures.

The present report discusses the results of an investigation of the penetration characteristics of spherical projectiles impacting a bed of fine particles of uniform size in a pressure environment which was varied from atmospheric to  $1 \times 10^{-5}$  mm Hg absolute. The penetration characteristics obtained through measurements and photographic techniques were examined to evaluate the effects of variations in the size of the test-bed particles, the testing technique, and several of the impacting body variables.

## SYMBOLS

|   |   |
|---|---|
| d | diameter of impacting projectile, cm          |
| k | penetration parameter                         |
| m | mass of impacting projectile, grams           |
| V | velocity of impacting projectile, meters/sec  |
| y | penetration depth of impacting projectile, cm |

## APPARATUS AND TEST PROCEDURE

### Apparatus

Description of projectiles and test-bed material.-- The impacting projectiles used in these penetration tests consisted of six spheres which varied in diameter from 1.59 to 2.54 centimeters and in mass from 12.3 to 66.7 grams. The mass and diameter of each of the spheres are listed in table I. The basic structure of each sphere was steel except for the lightest (configuration 4) which was made of plastic. Configurations of the same diameter but of different mass were obtained by boring desired amounts of steel from the spheres and replacing the removed volume with contoured balsa plugs. The chosen test configurations permitted the isolation and study of the separate effects of projectile mass and diameter on the penetration characteristics in the test-bed material.

The test-bed material on to which the projectiles were impacted consisted of aluminum oxide (Alumina) particles of uniform size. The average particle sizes used in these tests are listed in table II together with the average density of the material under atmospheric conditions prior to testing. The test-bed material varied from the granular consistency of the 600-micron particles to the fine powdery texture of the 3-micron particles. All particle sizes had been graded in accordance with the allowable sizing limits of reference 11. Aluminum oxide was chosen as the test-bed material because it is commercially available in large quantities of well-defined particle sizes, and because it is a dielectric (radar studies of the lunar surface, such as reference 8, suggest that the surface layer is a nonconducting material). In addition, aluminum oxide outgasses at a low rate and therefore can be economically subjected to low vacuum pressures. The densities listed in table II represent the average bulk densities for the different particle sizes which, because of the separation of particles, are significantly



less than the particle density of 3.95 grams per cubic centimeter. Several impact tests were also made on to a bed of silicon carbide (particle density of 3.20 grams per cubic centimeter), having an average particle size of 16 microns and an atmospheric bulk density of 1.16 grams per cubic centimeter, in an effort to study penetration characteristics in a different material.

Description of environmental chambers.- The penetration tests were performed in two environmental chambers which provided overlapping ranges of vacuum pressures. Both chambers utilized the same evacuation system, which consisted of a displacement pump with a free-air capacity of 425 liters per minute and a three-stage diffusion pump. The tests at atmospheric and intermediate vacuum pressures were conducted in a  $1\frac{1}{2}$ -cubic-foot (42.5 liters) stainless-steel chamber, shown schematically in figure 1. The chamber was connected to the pumping system by means of a  $1\frac{1}{4}$ -inch flexible bronze bellows and the pressures were measured by a vacuum gage capable of sensing pressures from atmospheric to  $2 \times 10^{-4}$  mm Hg. The top and one wall of the chamber were fitted with glass windows to permit visual and photographic observations of the contained test bed. Access to the test bed was provided by means of a removable top which, during reduced-pressure operations, was sealed to the chamber by an "O" ring. The removable top was equipped with a mechanism which housed, separately, as many as six projectiles and a mechanical link which was used to actuate the release mechanism of each housing. Impact velocities up to 2.44 meters/second could be obtained during free fall of the projectiles by adjusting the height of the housing mechanism above the test bed. Higher impact velocities could be achieved by removing the housing mechanism and replacing the mechanical link with a desired length of pipe equipped at the upper end with a mechanism to house and release a single projectile.

Vacuum pressures approaching  $5 \times 10^{-6}$  mm Hg were obtained by use of a Pyrex bell jar chamber having a nominal diameter of 18 inches and a height of 30 inches. This chamber, like most laboratory-type vacuum systems, was seated directly above the pumping apparatus and was equipped with two types of pressure-sensing devices: a thermocouple accessory circuit for measuring pressures between 1 and  $1 \times 10^{-2}$  mm Hg and an ionization gage which operates at pressures varying from  $1 \times 10^{-3}$  to  $2 \times 10^{-9}$  mm Hg. A brass container capable of holding approximately 0.3 cubic foot of test-bed material was mounted on a stand within the chamber as shown in the photograph of figure 2. The height of the container above the base of the bell jar was varied to obtain the desired impact velocity of the free-falling projectile. A single projectile was suspended from the top of the jar by means of an external permanent magnet and released as required by removal of the magnet. This chamber permitted free-fall impact velocities up to about 3.35 meters/second.

#### Test Procedure

The test procedure consisted of impacting spherical projectiles on to test beds composed of uniformly sized particles exposed to known vacuum pressures and recording the resulting penetration characteristics. Tests were conducted in two

environmental chambers which permitted an evaluation of the penetration characteristics over a range of pressures from atmospheric to  $1 \times 10^{-5}$  mm Hg absolute. (Pressures referred to in this paper are absolute pressures.) Sufficient quantities of the test material were placed in each chamber to provide a depth between 12 and 15 centimeters (approximately 5 or 6 inches). In preparation for a test the test bed was stirred to remove all packing effects and afterwards leveled to provide a smooth impact surface. After the preparation of the material at atmospheric pressure, the impacting projectile or projectiles (depending upon the housing mechanism being employed) were installed, the chamber sealed, and evacuation of the air begun. Upon reaching the desired pressure level, the evacuation pumps were shut out of the system and the projectile released to impact the surface. The chamber was then returned to atmospheric pressure by bleeding, in most cases, dry nitrogen into the system. After desired photographs were taken, measurements of the distances from a reference level to the undisturbed surface adjacent to the impact region and to the top of the impacting body were made to establish the depth of penetration. These measurements were made with a sliding scale which permitted accuracy to within  $\pm 0.05$  centimeter. Although the level of the test bed appeared to remain unchanged during chamber evacuation, a slight decrease was noted during the return-to-atmosphere cycle of the tests on the powdery materials as a result of the increased pressure in the system. Measurements were made at atmospheric pressure after the change had occurred, but, since it appeared from observations that both the surface of the test bed and the projectile shifted downward in unison, this change is not reflected in the penetration measurements.

In addition to the evaluation of the penetration characteristics of the projectiles into test beds consisting of uniform particle sizes, tests were also conducted for variations in the testing technique and in the projectiles to establish their effect on the penetration depth. The procedure involved in all tests was identical except that, in evaluating the effects of surface packing, the test procedure was interrupted by the application of a static loading to the test-bed surface, in 5-pound increments, immediately prior to sealing the chamber.

## RESULTS AND DISCUSSION

The results of experimental studies on spherical projectiles impacting fine particles exposed to a vacuum environment are presented in figures 3 to 11. These figures include curves and photographs which describe the penetration characteristics of the impacting projectiles as a function of the environmental pressures. The penetration characteristics, as affected by the size of the particles, and variations in the testing technique and in the projectiles are reviewed and discussed in the subsequent sections.

### Effect of Test-Bed Particle Size

The possibility that the layer of dust on the lunar surface consists of particles having a uniform particle size is indeed remote. However, fundamental research on materials consisting of fine particles requires a knowledge of the

effect of particle size before the more obvious case of random-particle-size distribution is examined. In view of this, the penetration characteristics of a body impacting nine separate sizes of test particles were evaluated and the results are presented in figures 3 to 7. Figure 3 presents the measured penetration depths for a spherical projectile as a function of the environmental pressure at the impact surface. Penetration data are included for average particle sizes ranging from 3 to 600 microns over a range of pressures between atmospheric and approximately  $1 \times 10^{-5}$  mm Hg. The figure shows that, within the limits of the investigation, the depth of penetration into particle sizes equal to or greater than 32 microns (particles having an obvious granular consistency) is independent of the environmental pressure. However, for particle sizes less than 32 microns (powdery in nature) the depth of penetration decreases rapidly with decreasing environmental pressure until the pressure is reduced to about 1 mm Hg. For pressures less than 1 mm Hg the penetration depth remains constant throughout the range of pressures investigated. Figure 3 further indicates that the depth of penetration in the coarse or granular particles is apparently unaffected by particle size whereas the penetration in the powdery materials increases with decreasing particle size.

The mechanisms involved in producing these penetration characteristics were examined by means of motion pictures taken during the impact process. Sequences taken from these movies are presented in figures 4 to 7, which show impacts into both granular and powdery materials at two different environmental pressures, atmospheric and 0.1 mm Hg. The reader is reminded that the depth of penetration, as indicated in figure 3, is independent of the environmental pressure for all pressures less than 1 mm Hg.

Figures 4 and 5 show impacts at atmospheric pressure and at a pressure of 0.1 mm Hg, respectively, on to a test bed consisting of particles having an average size of 600 microns. A comparison of the two figures reveals no apparent change in the impact phenomena due to the vacuum environment. This is also in accord with the penetration data of figure 3.

Figures 6 and 7 show the results of similar impacts on to a bed of particles having an average size of 16 microns. Figure 6, which depicts the impact under an atmospheric environment, shows the formation of a deep crater with an accompanying expulsion of the dust in small clusters. In the photographs of figure 7, the test conditions are identical to those employed in obtaining figure 6 except that the pressure has been reduced to 0.1 mm Hg. It is noted in this case that upon impact, instead of creating the explosive crater associated with atmospheric impacts such as illustrated by figure 6, the body penetrated the surface and was essentially enveloped by the dust. It was observed in the course of these tests on the powdery material that, as the system pressure is reduced from atmospheric, the number of particles expelled decreases until, at pressures of approximately 1 mm Hg and lower, no expulsion is evident.

A possible explanation of the behavior of the different particle sizes of the test-bed material during the impact process is afforded by an examination of the manner in which the energy of the impacting body is dissipated. In general, the body energy is primarily dissipated by packing of the material immediately ahead of the body and the expulsion or displacement of the particles. From a

consideration of these factors, it is apparent that for identical test conditions, penetration depths in the granular type materials should be less than those in the powdery type since the granular particles are less susceptible to packing and, because of their larger size and mass, offer greater resistance to particle displacement.

The particle-displacement characteristics, as illustrated in figures 4 to 7, can possibly be explained by examining certain forces associated with the individual particles. Particles displaced by the projectile possess inertial forces which are opposed by cohesive and frictional forces between particles. The inertial forces of granular materials apparently exceed the cohesive and frictional forces so that particles are displaced from the impact region. This appears to be the case regardless of the environmental pressure. On the other hand, for the powdery materials, the particle inertial force is apparently less dominant than the combined cohesive and frictional forces and such impacts, at low environmental pressures, result in no medium expulsion. However, in atmospheric and near-atmospheric pressure environments (pressures greater than about 1 mm Hg) the powdery particles are supplied sufficient inertia, because of the compression of air present within the test bed, to overcome the resisting cohesive and frictional forces and such impacts result in spectacular explosions of particle clusters.

#### Effect of Variation in Testing Technique

In view of the scatter noted in the penetration measurements of figure 3, several tests were made to evaluate possible scattering effects due to certain variables associated with the testing technique. These variables, some of which were examined in more detail than others, included the preparation of the test-bed material prior to testing, the depth of the test bed, the evacuation rate, and the duration of the partial-pressure environment.

Preparation of the test-bed material.- The data presented in figure 3 and illustrated by the photographs of figures 4 to 7 are the results of impacts on to a test bed which had been stirred to remove any packing effects. Additional data were obtained for two sizes of particles - one powdery (16 microns) and one granular (600 microns) - to evaluate any surface packing effects on the depth of penetration. Measurements made in the granular material appeared to be unaffected by surface packing, at least for static packing pressures up to approximately 150 grams per square centimeter, which indicates that, for such particle sizes, depth of penetration is not critically affected by the preparation techniques. The depth of penetration in the powdery material, on the other hand, appeared to be affected by inconsistencies inherent in the preparation process which suggested possible packing effects. The results of tests to investigate these possible packing effects in a powdery material are presented in figure 8 where the depth of penetration is plotted as a function of static packing pressure for impacts under both atmospheric and vacuum (0.8 mm Hg) environments. The static packing pressure was in all cases applied at atmospheric pressure prior to sealing the chamber and immediately following the normal preparation process. The data show that, in atmospheric and vacuum environments, the depth of penetration decreases with increasing packing pressure. It is also observed from the data that the rate

at which the depth of penetration decreases appears to be greater for the atmospheric than for the vacuum case. It is interesting to note that for extreme packing (accomplished by means of a dynamic loading which yielded a packing pressure far in excess of the pressure scale of fig. 8) the projectile penetrated the surface deeper in the vacuum environment than at atmospheric pressure.

References 8 and 9 present penetration results for test beds of mixed particle sizes in which the projectile generally penetrated the surface deeper in the vacuum environment than at atmospheric pressure. The penetration results presented in reference 9 were obtained for a slight amount of packing; whereas, those presented in reference 8 were apparently obtained for a nonpacked surface. Reference 10 presents penetration results for test beds of mixed particle sizes and shows that the depth of penetration is a function of surface packing. For an unpacked surface the projectile penetrates the surface deeper at atmospheric pressure than in the vacuum environment; however, for a slightly packed surface the projectile penetrates the surface deeper in the vacuum environment. The contrast in the degree of surface packing which yields deeper penetration in the vacuum environment is possibly due to the mixture of particle sizes in the reference cases, whereas the data of this paper were obtained by using a test bed of particles of uniform size.

The craters resulting from the impact of the projectile on the extremely packed (heavy static load) powdery surface in both atmospheric and vacuum environments are shown in the photographs of figure 9. This figure also includes photographs which illustrate the craters formed during the impact on the surface which had been in one case lightly packed (23.5 grams per square centimeter static packing pressure) and in another intermediate case, moderately packed (68 grams per square centimeter static packing pressure). For impacts at atmospheric pressure, the photographs show that less and less material is expelled from the impact crater as the packing pressure is increased, which is understandable since packing tends to enhance the coherency between particles and the larger clusters thereby formed become less susceptible to expulsion. The craters formed by impacts under a vacuum environment on packed surfaces, like those under atmospheric conditions, appear to resemble the craters formed during the impact on the nonpacked material. (See fig. 7.) The basic difference between the craters for this condition is the size of the particle clusters that compose the crater debris. The photographs show that, as the amount of packing is increased, the size of these clusters increases which again is believed to be due to the increased particle coherency.

Impacts for the extreme packing cases present an interesting crater phenomenon. In the atmospheric case the body came to rest partially imbedded in what appears to be an otherwise undisturbed surface, whereas in the vacuum case for the same packing, a crater composed of particle clusters in assorted sizes was formed. The reason for this dissimilarity has not been established. It was initially believed that this difference in the cratering resulted from a loosening of the surface brought about by the evacuation process. However, subsequent tests conducted at atmospheric pressure after the test bed had been subjected to a vacuum environment indicated no apparent differences in either penetration depth or crater formation when compared with the noncycled atmospheric pressure test. It

is felt that the explanation is to be sought on the molecular level with inter-particle forces of significance; the presence of water vapor and the degree of vacuum environment probably are also significant factors.

Depth of the test bed.- In an effort to evaluate the effects of the depth of the test-bed material on the penetration depth in the different sizes of particles, several of the impact tests which produced data for figure 3 were repeated on depths which differed from the 5- to 6-inch levels maintained for those data. Tests on the material indicate that the measured depth of penetration in the granular particles was unaffected by the depth of the test bed for all cases tested. These cases included penetration depths where the projectile came to rest at distances ranging from 1 diameter to over 4 diameters above the solid subsurface. Since a certain amount of the projectile energy is dissipated into packing the material in the advance path of the penetrating body and since the powdery material is more subject to packing than the granular material, the depth of penetration in the powdery material is more readily affected by the boundary condition afforded by the subsurface. It appears from the tests conducted on such particle sizes that, in order to avoid scatter due to boundary restrictions, a test bed of sufficient depth must be available to maintain a minimum distance of about  $1\frac{1}{2}$  diameters between the projectile following penetration and the hard subsurface.

Evacuation rate.- The application of the partial-pressure environment to the test chamber depends on manual control of the valving system and, as such, leads to variations in the evacuation or pumping rate. The effect of such variations on penetration depths was examined. The results of these tests indicate that, except for depth of penetration at pressures approaching atmospheric in the powdery material, the penetration depth is apparently unaffected by the evacuation rate. At near-atmospheric pressures it appears that the slower the pumping rate the deeper the penetration in the powdery material, possibly because of the fact that the higher pumping rates, by virtue of the rapid expulsion of the trapped air between particles (evident from visible spouting of the particles), tend to increase the density of the test bed and hence retard penetration.

Exposure time in environment.- During the course of the tests, particularly in the high vacuum region, the test bed was exposed to the test environment for random durations of time. Variations in the depth of penetration due to exposure of the material to a given pressure, for times which in some cases extended up to approximately 24 hours, appeared to be insignificant since the measured penetration depths for such cases fell within the normal range of scatter of the data. However, it was noted during tests on the powdery material that altering the test technique prior to impact to include cycling, that is, impacting the projectile after reducing the pressure below the test environment and returning, affected the results by reducing the penetration depth. This decrease in penetration following a pressure cycling period may be a factor in the differences noted in the trends of the data of this paper and that of reference 9 where data at all pressure levels were obtained following a vacuum of  $1 \times 10^{-5}$  mm Hg.

## Effect of Projectile Variables

The data of figures 3 to 9 present the penetration characteristics of 2.54-centimeter, 66.7-gram spherical projectiles impacting a test bed as affected by variables associated with the materials and environment of the test bed. Tests were also conducted to evaluate the effects of certain projectile variables. The results of these tests are presented in figure 10, where the depth of penetration in a granular and a powdery material is presented as a function of environmental pressure showing the effect of projectile mass, diameter, and impact velocity. Figure 10 shows that the penetration depth in the granular material, over the entire pressure range, and in the powdery material, below environmental pressures of 1 mm Hg, can, in general, be related to these variables by means of the empirical expression:

$$y = k \frac{m^{1/2} v^{2/3}}{d}$$

The penetration parameter  $k$  for each of the various particle sizes of the test-bed material was evaluated from the experimental data by expressing as a ratio the depth of penetration of the test configuration and the corresponding projectile variables as contained in the empirical expression. Values of this parameter, based upon the penetration depth which best faired the data at pressures below 1 mm Hg, are presented as a function of average particle size in figure 11. Figure 11 is a composite of all tests conducted on the aluminum oxide particle sizes of table II and includes the range of projectile variables (mass, diameter, and impact velocity) as contained in table I and figure 10. Figure 11 also includes data obtained experimentally from the impact of one configuration on a test bed consisting of 5-micron particles (not listed in table II) and from impacts on two other materials, silicon carbide and dry sand. The data from the impact of three configurations in 16-micron silicon carbide were obtained in the course of the tests on aluminum oxide, whereas that for dry sand was obtained from reference 6 which presents an identical empirical expression for penetration depths resulting from impacts of projectiles having a much wider range of test variables than those presented here. The data for the dry sand were obtained at atmospheric pressure but are included here because penetration depths in granular materials appear to be independent of the environmental pressure.

Figure 11 shows that the penetration parameter  $k$  is essentially constant for particles varying in size from 600 microns (the largest size examined) to approximately 32 microns. For particle sizes less than 32 microns, the values of  $k$  rapidly increase in the region of transition from granular to powdery types and gradually increase with further decreases in the particle size. The measured values of  $k$  for powdery silicon carbide and dry granular sand appear to be in agreement with the faired aluminum oxide data. It appears, therefore, that the depth of penetration of spherical projectiles in granular materials (particle sizes greater than approximately 32 microns) can be described by the expression

$$y = 0.44 \frac{m^{1/2} v^{2/3}}{d}$$

whereas the depth of penetration in powdery materials (particle sizes less than approximately 32 microns) is a function of both the projectile variables and the particle size.

## CONCLUSIONS

The results of an experimental investigation of the penetration characteristics of spherical projectiles impacting on to a test bed of fine particles, uniform in size, and under a pressure environment which ranged from atmospheric to  $1 \times 10^{-5}$  mm Hg suggest the following conclusions:

1. The depth of penetration into beds of aluminum oxide particles ranging in size from 600 microns (the largest size investigated) to about 32 microns is independent of both the environmental pressure and the average particle size. For impacts on to particles smaller than 32 microns, the depth of penetration increases with decreasing particle size and is dependent upon the environmental pressure in the range between atmospheric and approximately 1 mm Hg. High-speed motion pictures of the impacts showed that the behavior of the granular particles (particles whose average size was 32 microns or larger) was unaffected by environmental pressures. However, for smaller particles, which are powdery in nature, it was observed that the number of particles expelled during the impact process decreased as the pressure was reduced from atmospheric to approximately 1 mm Hg. No expulsion was evident at lower pressures.

2. Penetration depths in the granular materials are unaffected by surface packing for static packing pressures up to approximately 150 grams per square centimeter; however, packing of the powdery materials results in a significant effect on the penetration depth of projectiles at both atmospheric and vacuum pressures. Since packing appears to occur primarily in the vicinity immediately ahead of the projectile in the penetration process, test beds of powdery materials must be deeper than those of granular materials to avoid effects of the subsurface on penetration. However, within the scope of the tests reported herein, penetration depths of projectiles into all sizes of particles are unaffected by either pumping rate or the exposure time of the test bed to the pressure environment.

3. An empirical expression was formulated from the experimental results which relates the depth of penetration to certain projectile variables for impacts on to the granular material over the entire range of test pressure and for impacts on to powdery materials below environmental pressures of 1 mm Hg. As anticipated, an increase in projectile mass or impact velocity and a decrease in body diameter results in an increase in the depth of penetration.

Langley Research Center,  
National Aeronautics and Space Administration,  
Langley Station, Hampton, Va., September 18, 1962.



## REFERENCES

1. Urey, Harold C.: The Origin of the Moon's Surface Features. Reprinted from *Sky and Telescope*, vol. XV, nos. 3 and 4, Jan.-Feb., 1956.
2. Gold, Thomas: Dust on the Moon. Vol. II of *Vistas in Astronautics*, Morton Alperin and Hollingsworth F. Gregory, eds., Pergamon Press (New York), 1959, pp. 261-266.
3. Whipple, Fred L.: On the Lunar Dust Layer. Vol. II of *Vistas in Astronautics*, Morton Alperin and Hollingsworth F. Gregory, eds., Pergamon Press (New York), 1959, pp. 267-272.
4. Hapke, Bruce W.: Preliminary Report on Experiments Relating to the Lunar Surface. Contract NsG 119-61, Center for Radiophysics and Space Res., Cornell Univ., Sept. 1961.
5. Salisbury, John W., and Campen, Charles F., Jr.: Location of a Lunar Base. GRD Res. Notes No. 70 (AFCRL 870) Air Force Cambridge Res. Labs., Oct. 1961.
6. McCarty, John Locke, and Carden, Huey D.: Impact Characteristics of Various Materials Obtained by an Acceleration-Time-History Technique Applicable to Evaluating Remote Targets. NASA TN D-1269, 1962.
7. Green, Jack: The Physical Characteristics of the Lunar Surface. *Proc. Lunar and Planetary Exploration Colloquium*, vol. 1, no. 1, May 13, 1958, pp. 11-15.
8. Brunschwig, M., Fensler, W. E., et al.: Estimation of the Physical Constants of the Lunar Surface. Rep. 3544-1-F, College Eng., Univ. of Michigan, Nov. 1960.
9. Geer, Richard Lansing: Impact Studies on Lunar Dust Models at Various Vacuums. ASD Tech. Rep. 61-595, U.S. Air Force, Jan. 1962.
10. Roddy, David J., Rittenhouse, John B., and Scott, Ronald F.: Dynamic Penetration Studies in Crushed Rock Under Atmospheric and Vacuum Conditions. Tech. Rep. No. 32-242 (Contract NAS 7-100), Jet Propulsion Lab., C.I.T., Apr. 6, 1962.
11. Anon.: Abrasive Grain Sizes. Simplified Practice Recommendation 118-50, U.S. Dept. of Commerce, June 1, 1950.

TABLE I.- DESCRIPTION OF SPHERICAL PROJECTILES

| Configuration | Diameter,<br>cm | Mass,<br>g |
|---------------|-----------------|------------|
| 1             | 2.54            | 66.7       |
| 2             | 2.54            | 47.4       |
| 3             | 2.54            | 16.4       |
| 4             | 2.54            | 12.3       |
| 5             | 1.91            | 16.4       |
| 6             | 1.59            | 16.4       |

TABLE II.- CHARACTERISTICS OF TEST-BED MATERIAL

| Average particle size,<br>microns | Average bulk density,<br>g/cc |
|-----------------------------------|-------------------------------|
| 600                               | 2.14                          |
| 266                               | 2.10                          |
| 86                                | 2.06                          |
| 44                                | 1.84                          |
| 32                                | 1.78                          |
| 23                                | 1.67                          |
| 16                                | 1.44                          |
| 8                                 | 1.27                          |
| 3                                 | .97                           |

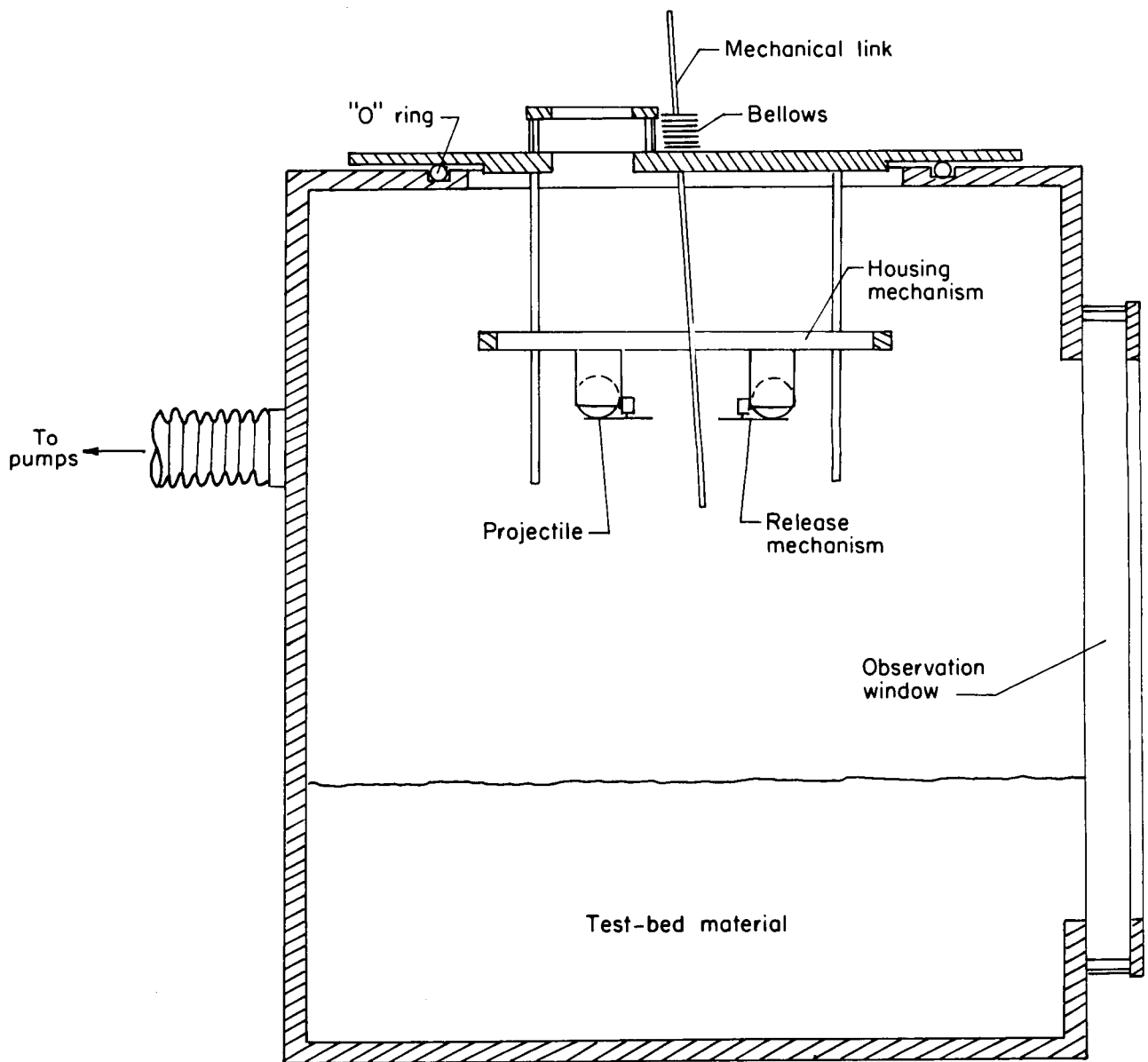
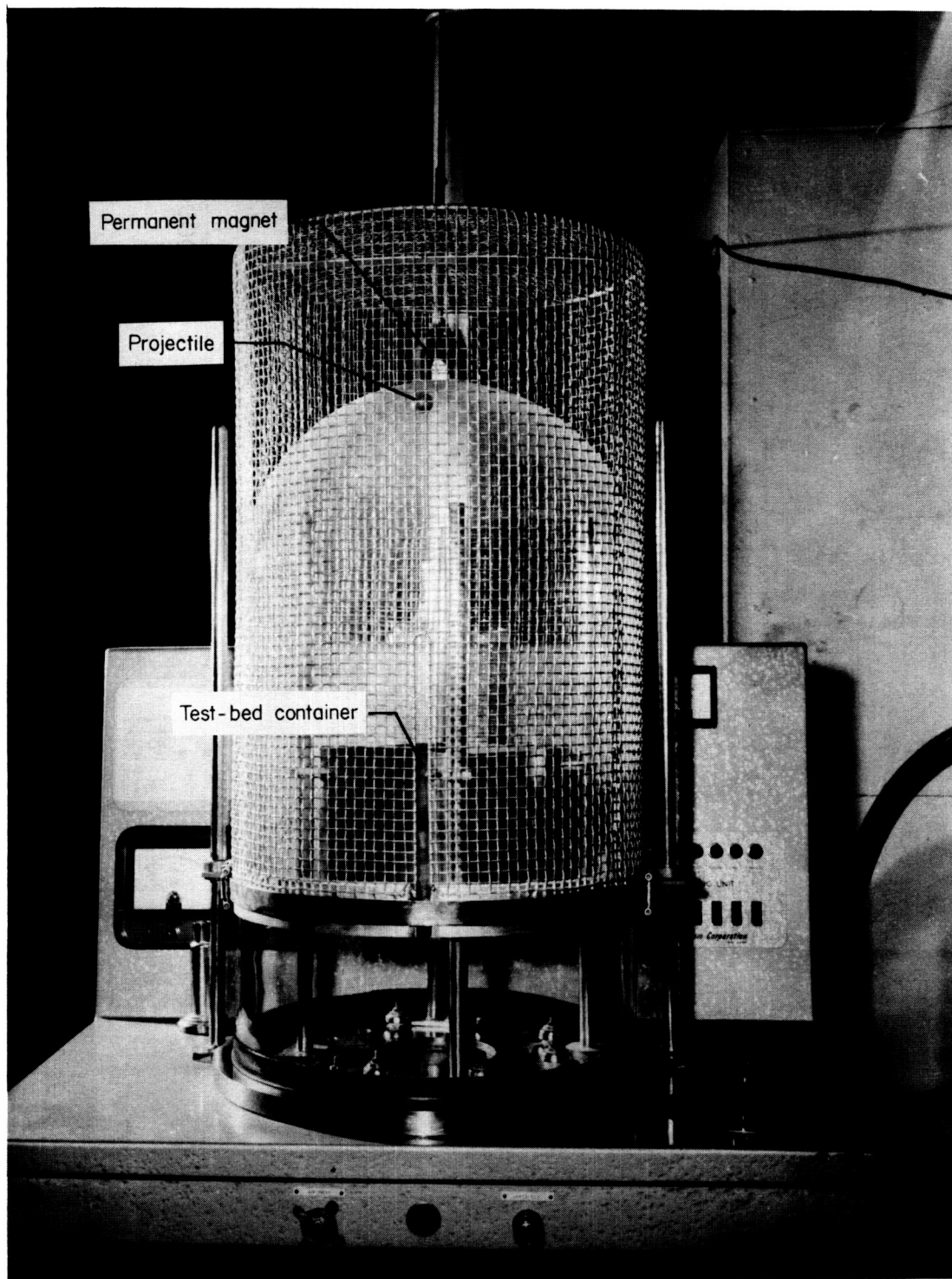


Figure 1.- Sectional sketch of low-vacuum environmental chamber showing pertinent components.



L-62-3851.1

Figure 2.- High-vacuum environmental chamber and test apparatus.

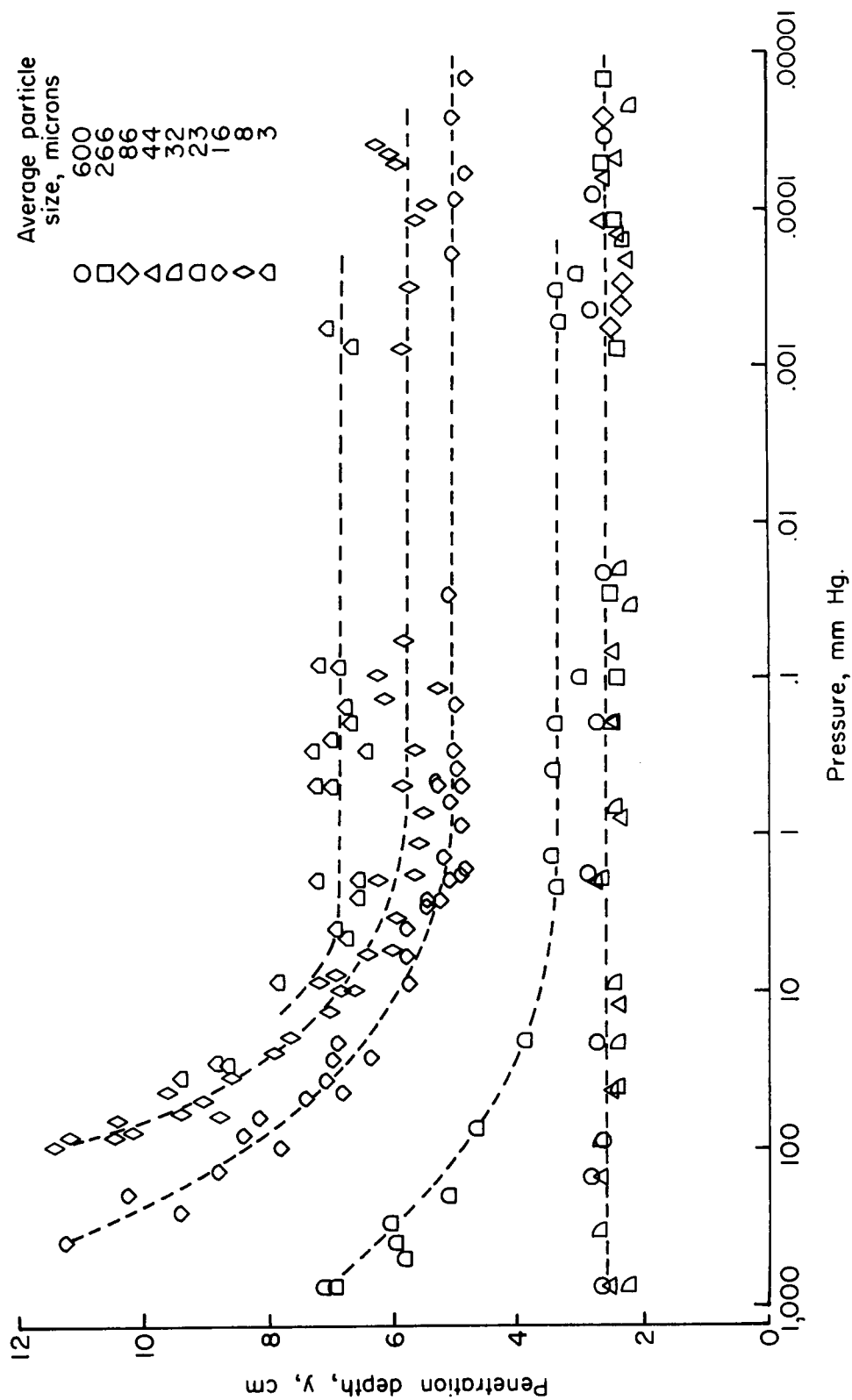
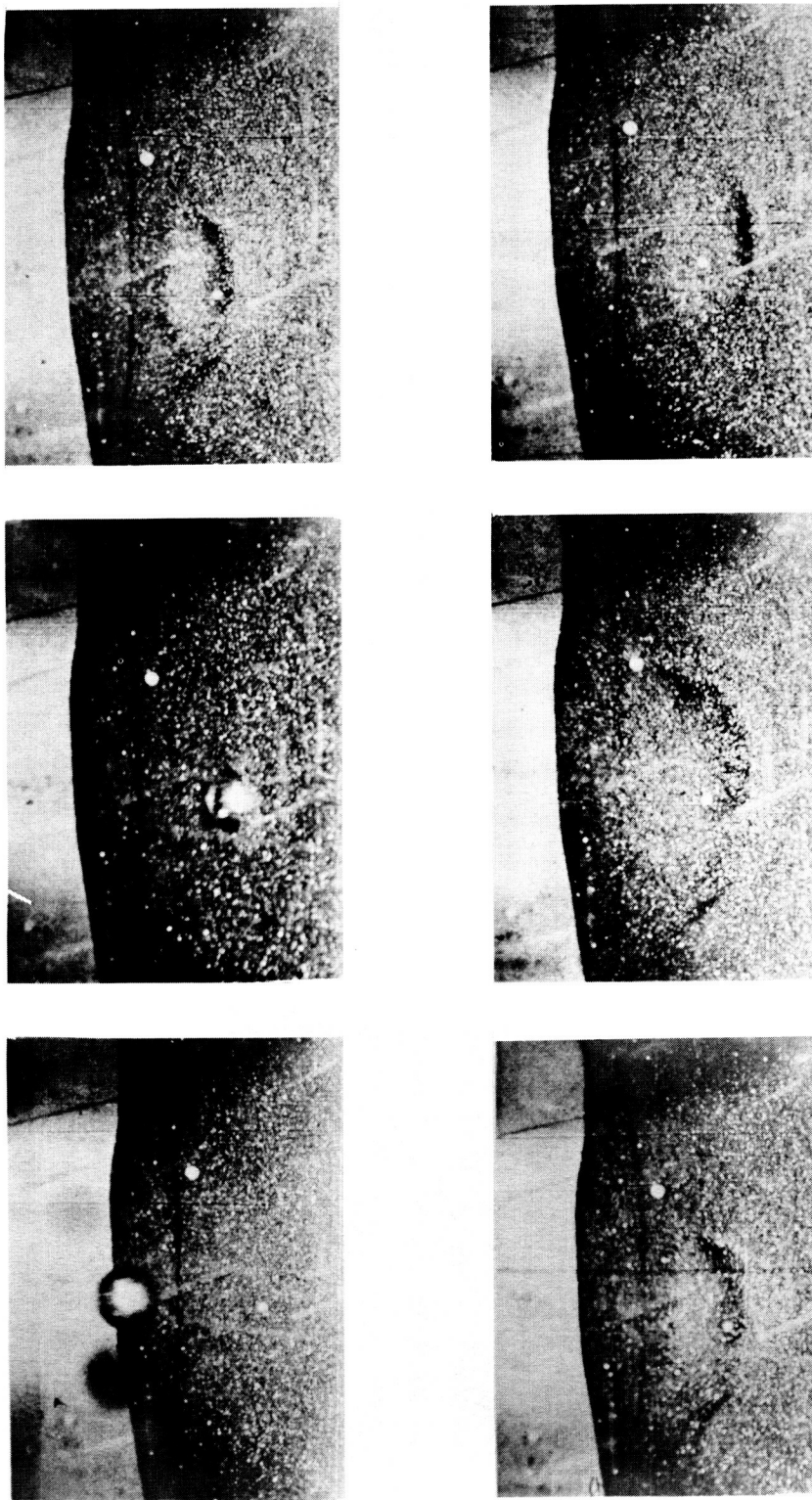


Figure 3.-- Effect of vacuum pressures on penetration depths in different sizes of fine particles.  
 $m = 66.7$  grams;  $d = 2.54$  centimeters;  $V = 2.44$  meters per second.



L-62-3958

Figure 4.- Sequence of photographs showing a projectile impacting 600-micron particles at atmospheric pressure.  $m = 66.7$  grams;  $d = 2.54$  centimeters;  $V = 4.55$  meters per second.

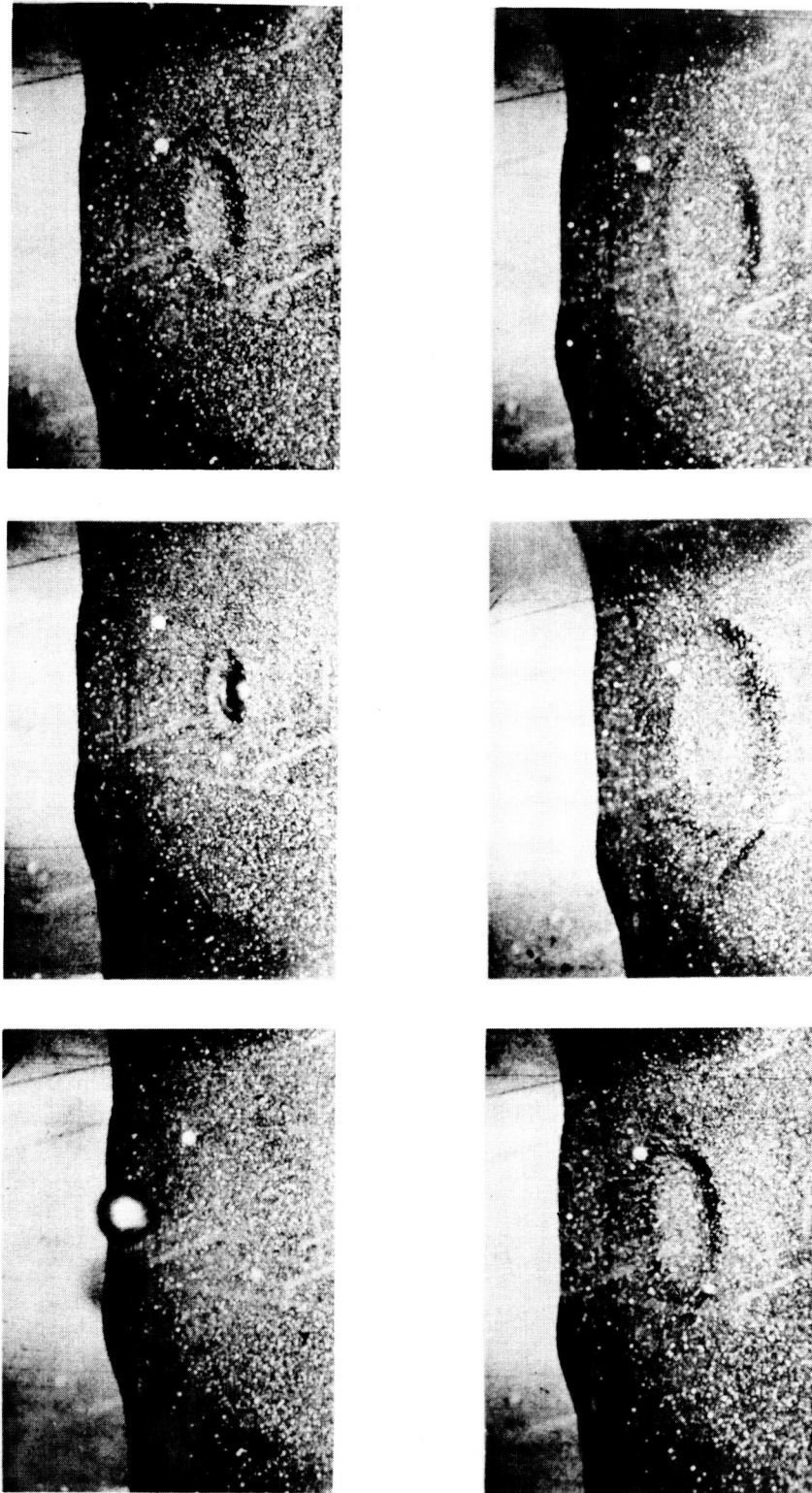
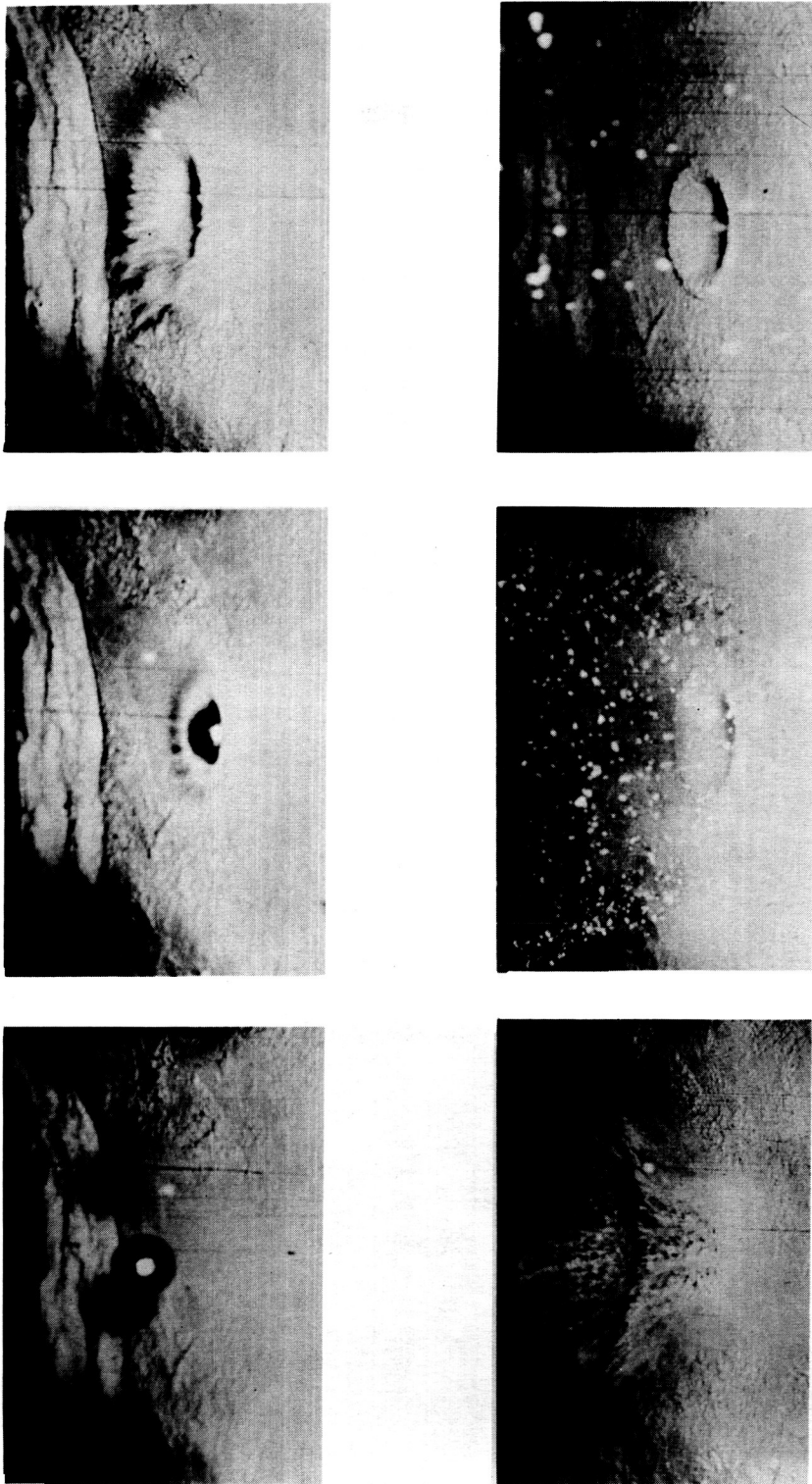
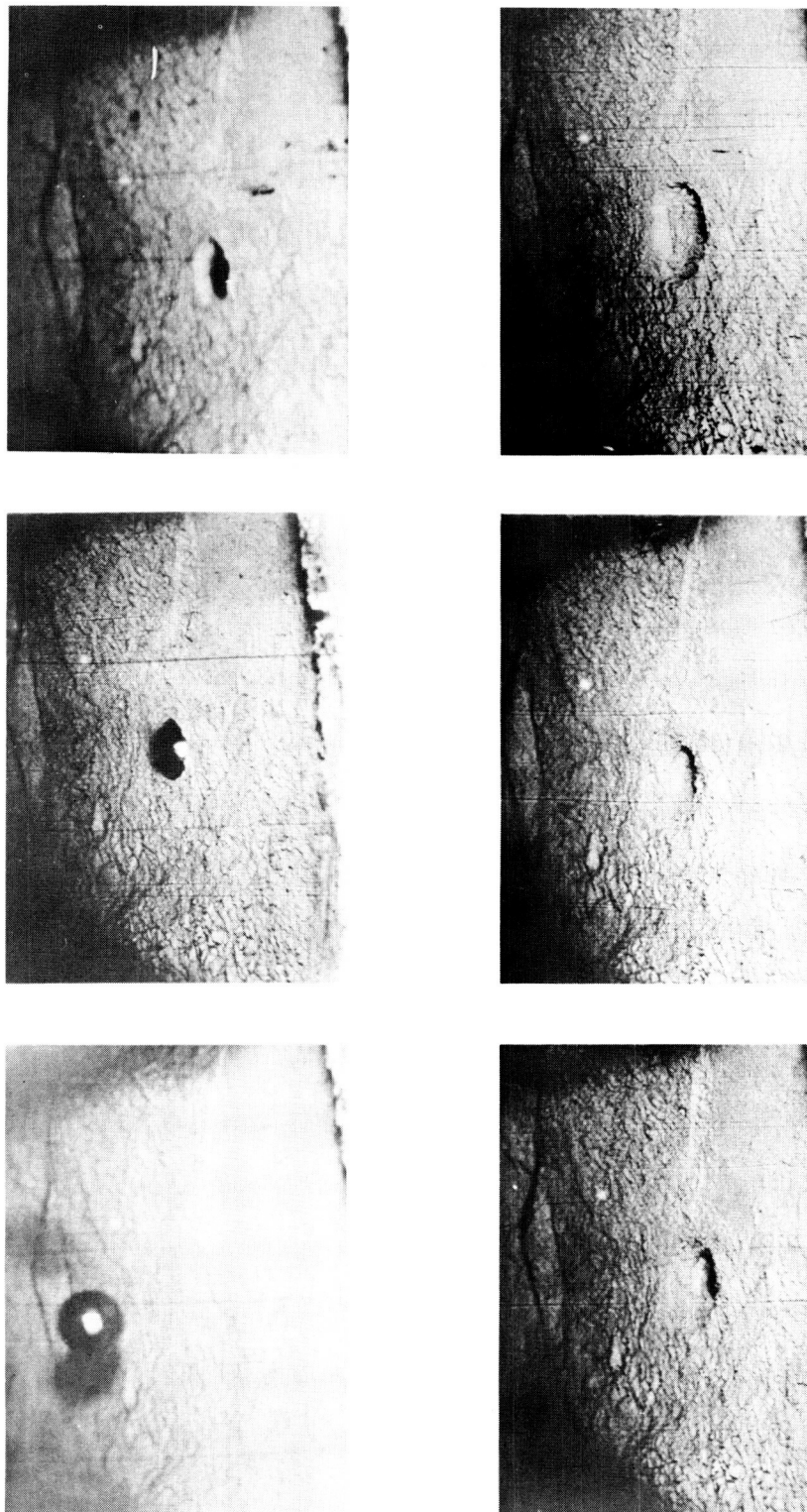


Figure 5.- Sequence of photographs showing a projectile impacting 600-micron particles at  
 0.1 mm Hg pressure.  $m = 66.7$  grams;  $d = 2.54$  centimeters;  $V = 4.55$  meters per second.



I-62-3956  
 Figure 6.- Sequence of photographs showing a projectile impacting 16-micron particles at  
 atmospheric pressure.  $m = 66.7$  grams;  $d = 2.54$  centimeters;  $V = 4.55$  meters per second.





L-62-3957

Figure 7.- Sequence of photographs showing a projectile impacting 16-micron particles at 0.1 mm Hg pressure.  $m = 66.7$  grams;  $d = 2.54$  centimeters;  $V = 4.55$  meters per second.

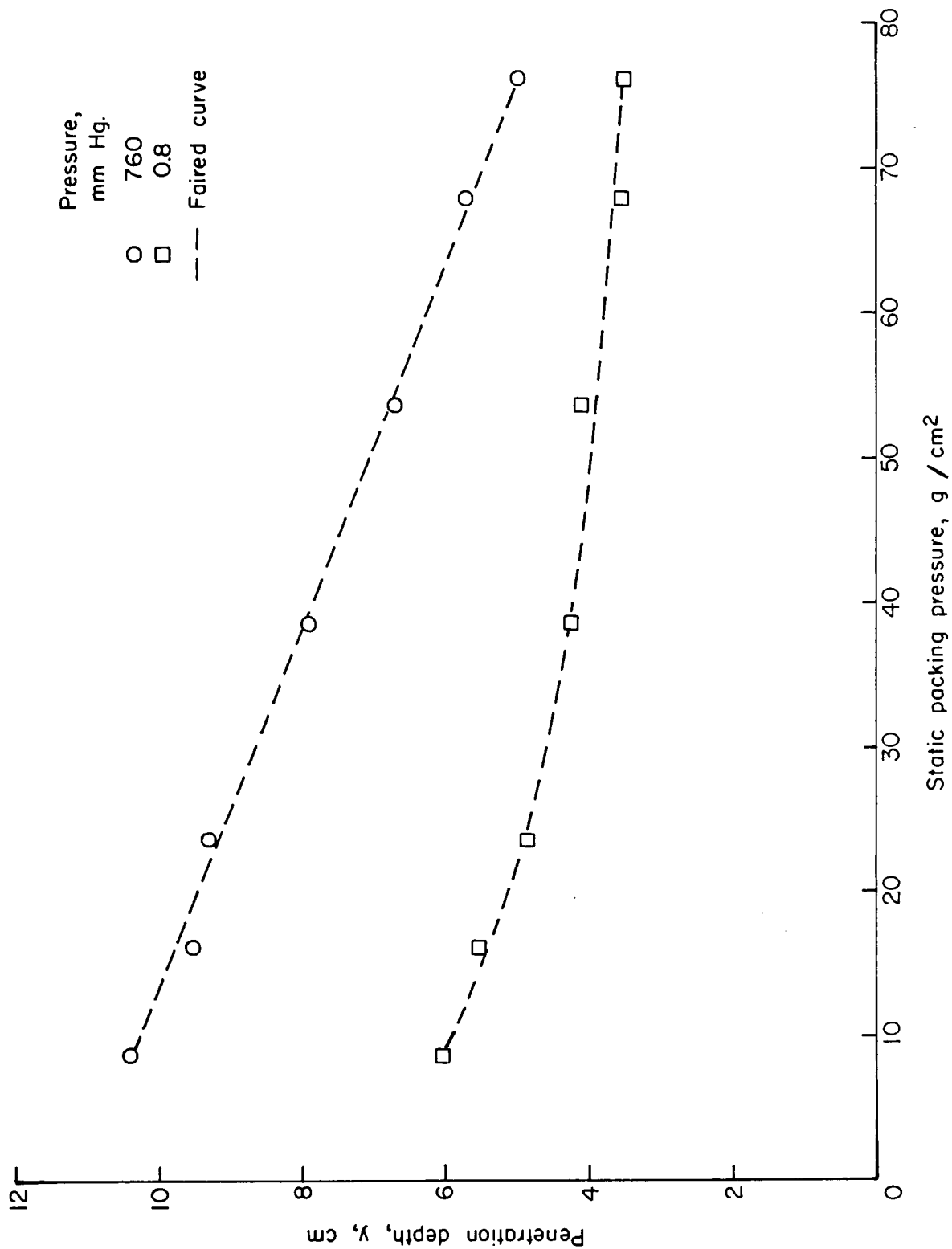
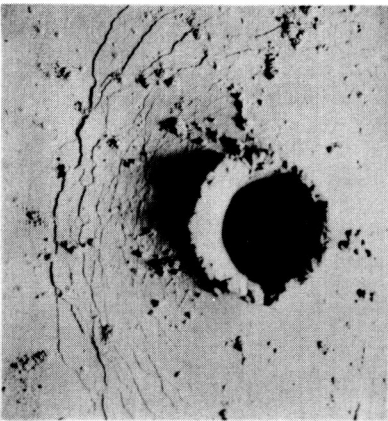
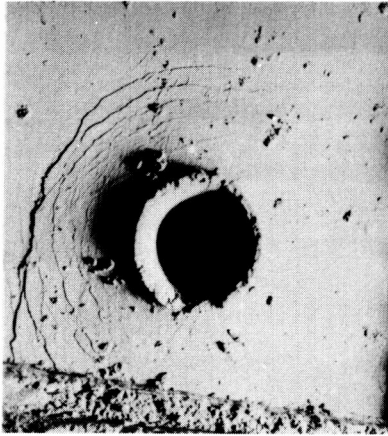


Figure 8.- Effect of packing on penetration depths in 16-micron particles.  $m = 66.7$  grams;  
 $d = 2.54$  centimeters;  $V = 4.48$  meters per second.

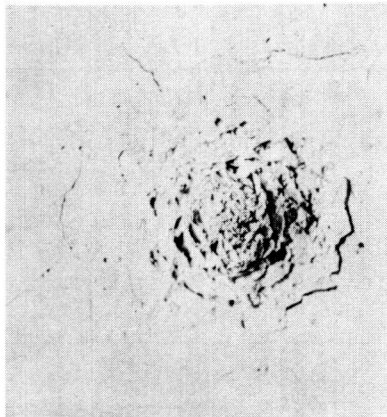


Light packing

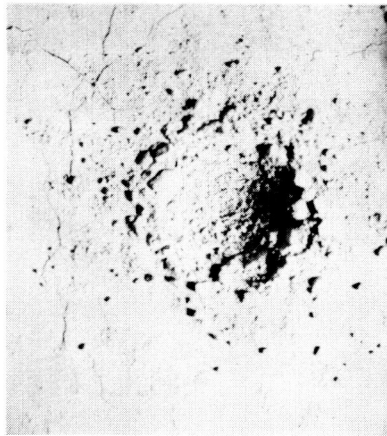


Moderate packing

(a) Atmospheric pressure.

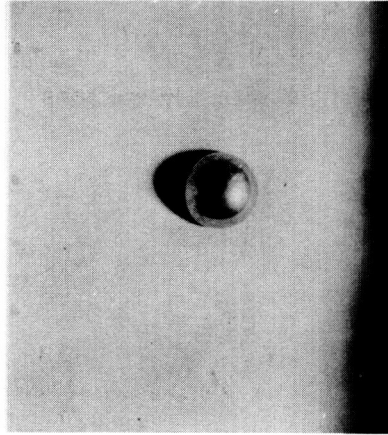


Light packing

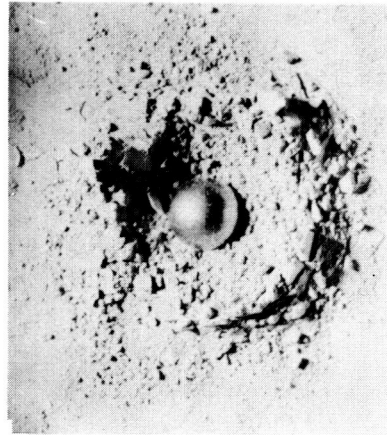


Moderate packing

(b) Vacuum pressure (0.8 mm Hg).



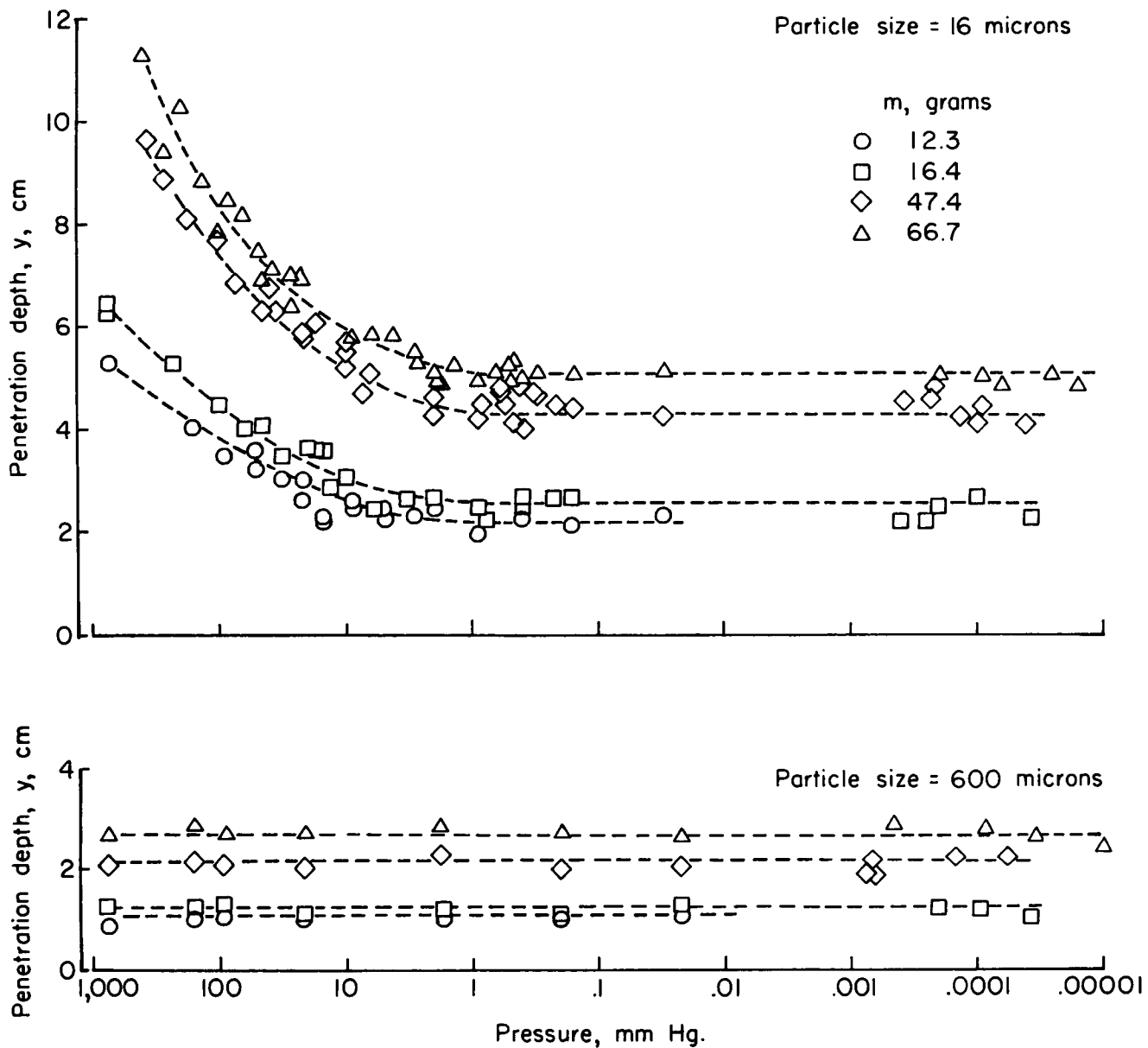
Extreme packing



Extreme packing

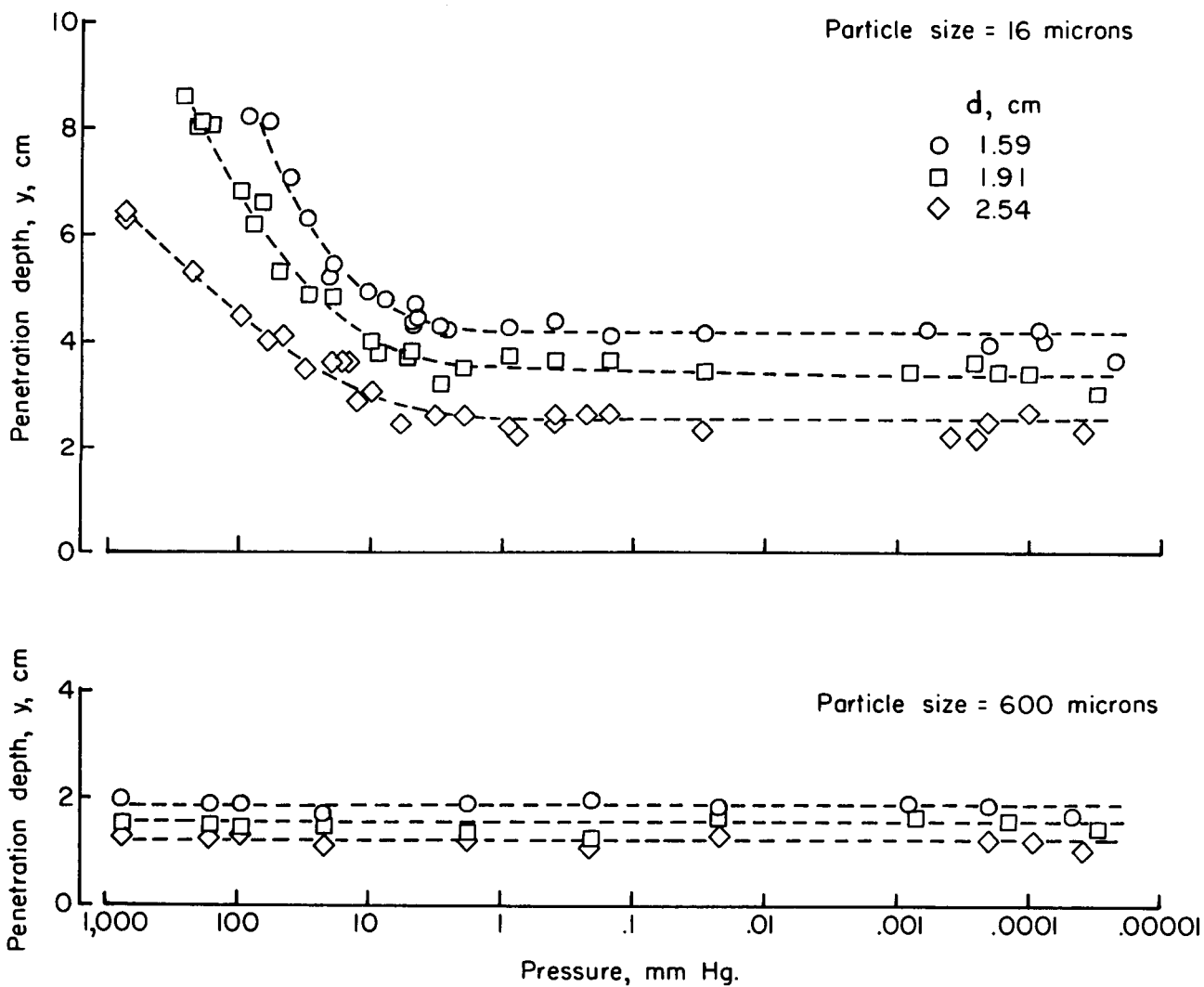
L-62-3959.1

Figure 9.- Photographs of craters resulting from impacts on packed test beds of 16-micron particles.  
 $m = 66.7$  grams;  $d = 2.54$  centimeters;  $V = 4.48$  meters per second.



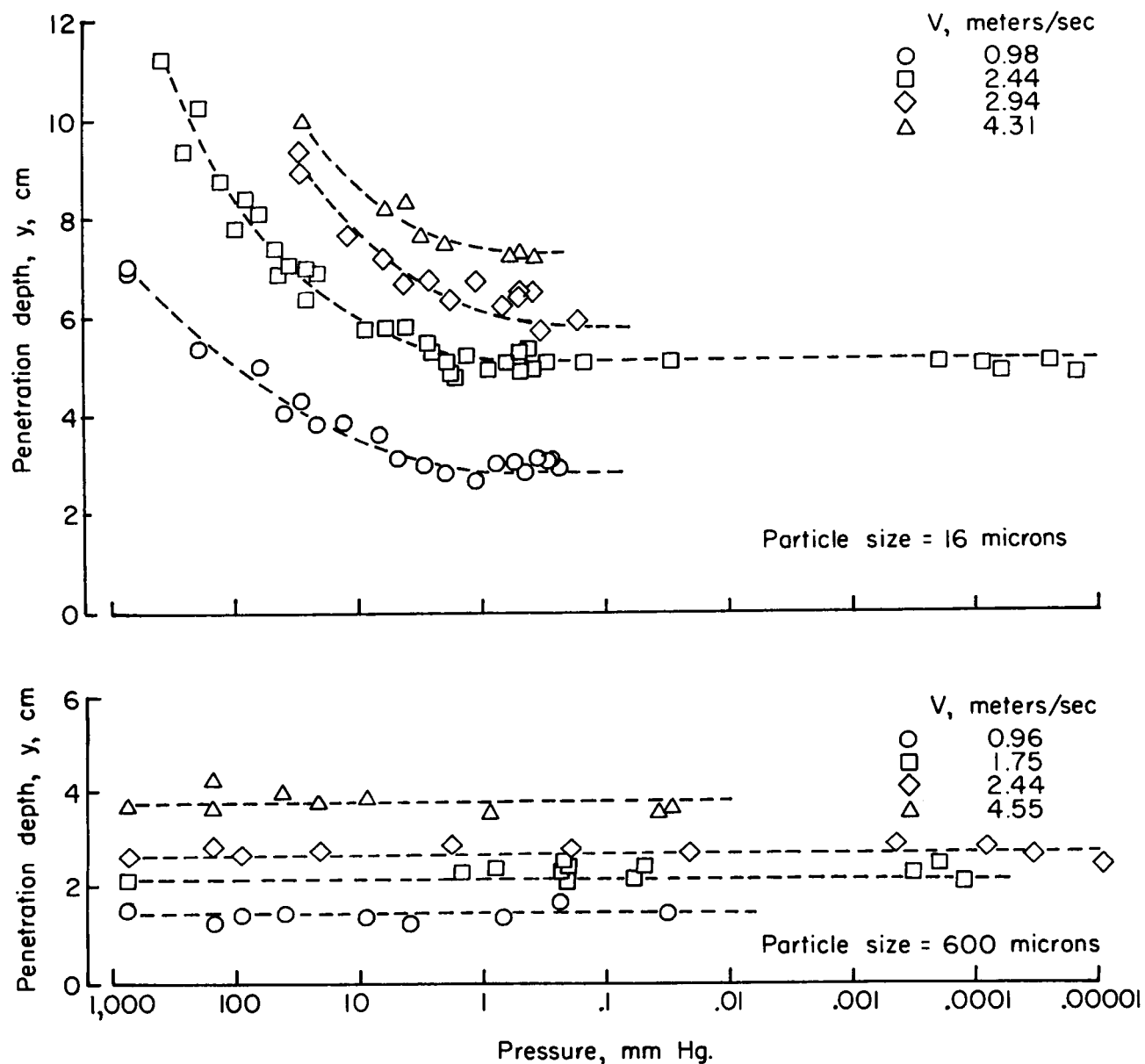
(a) Mass.  $d = 2.54$  centimeters;  $V = 2.44$  meters per second.

Figure 10.- Effect of projectile variables on depth of penetration.



(b) Diameter.  $m = 66.7$  grams;  $V = 2.44$  meters per second.

Figure 10.- Continued.



(c) Velocity.  $m = 66.7$  grams;  $d = 2.54$  centimeters.

Figure 10.- Concluded.

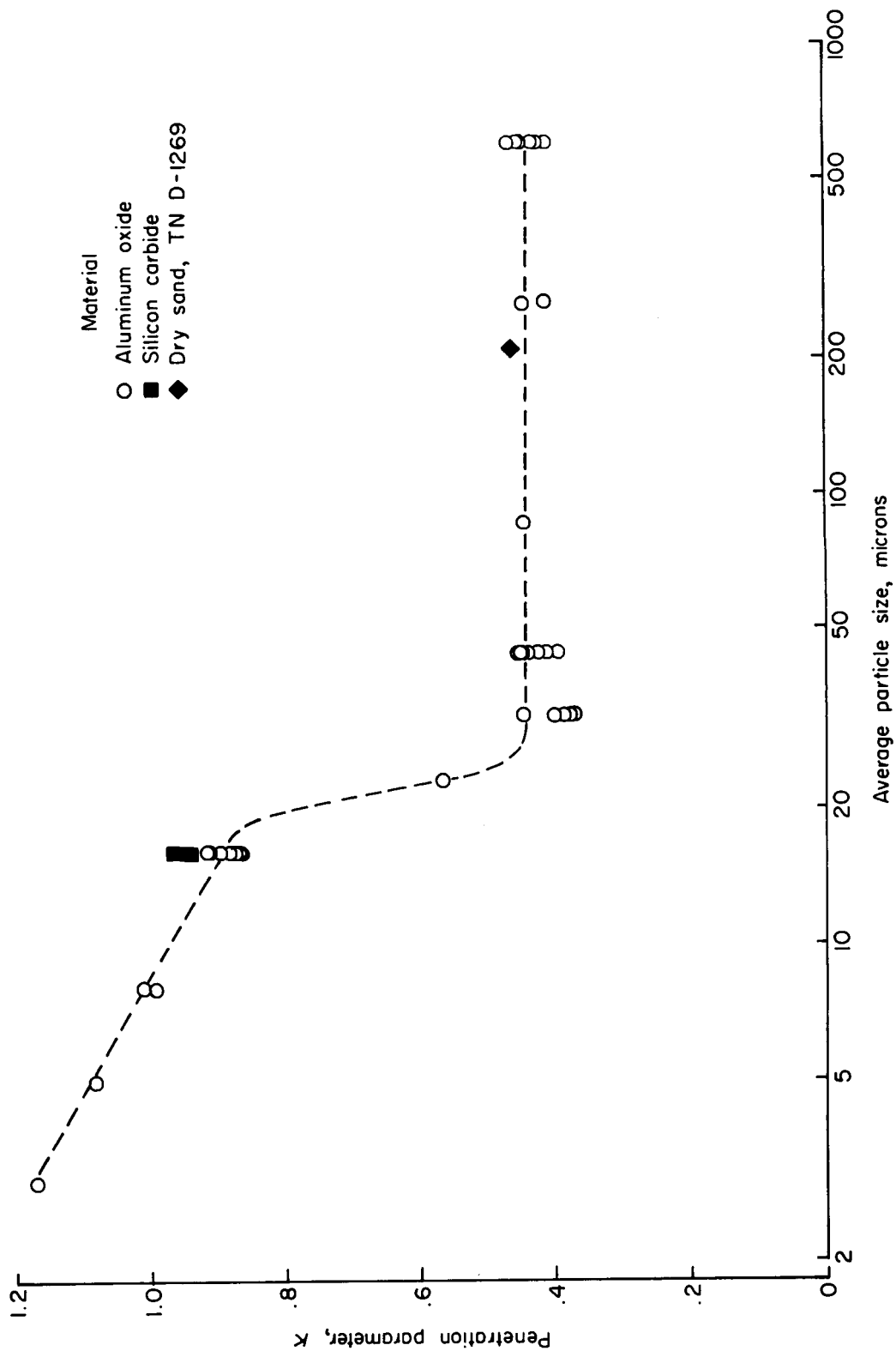


Figure 11.- Effect of particle size on penetration parameter. Pressure < 1 mm Hg.  $k = \frac{y}{\frac{m^1/2v^2/3}{d}}$